

NUMERICAL STUDY OF EFFECT OF ROUGHNESS ON POROUS LONG JOURNAL BEARING WITH HETEROGENEOUS SURFACE

G. K. KALAVATHI¹, P. A. DINESH and K. GURURAJAN

ABSTRACT. The present paper describes the numerical study of surface roughness effects on infinitely long journal bearing with slip/no-slip surfaces. Christensen stochastic theory is adopted to study the effect of roughness. The governing equations are obtained by considering suitable boundary conditions and which are found to be non-linear partial differential equations and are solved using numerical method. To find the angle of cavitation, Regula-falsi method is used. The Gaussian 16-point formula is used to estimate load carrying capacity, attitude angle, friction and coefficient of friction. It was found that surface roughness effect is more dominant for the long bearing approximation and the influence of longitudinal and transverse roughness is in reverse trend. Further, attitude angle decreases as compared to smooth for transverse roughness whereas it is insignificant for longitudinal roughness. It is observed that, as a particular, results of infinitely long journal bearing are significantly different than those for the narrow journal bearing.

Keywords and phrases: Heterogeneous slip/no-slip surface, Long journal bearing, Porous, Surface roughness.

1. INTRODUCTION

The assumption that the linguistic studies of hydrodynamically lubricated machines are smooth is unrealistic for a bearing operating with small film thickness. This is because, in practice, all the surfaces have irregularities. Also, the surface irregularity height will be of same order as the mean separation between lubricated contacts. Tzeng and Saibel [1, 2] were the first who have studied the surface roughness effects on a slider bearing and narrow journal bearing surface in hydrodynamic theory. Christensen [3] has developed a stochastic theory for hydrodynamic lubrication of rough surfaces. Patir et al. [4], Turga et al. [5], and Gururajan et al. [6, 7, 8, 9, 10] have extended this theory to study roughness

Received by the editors December 03, 2015; Revised: July 02, 2016; Accepted: July 09, 2016

¹corresponding author

effects on the performance of bearing characteristics. It was found that direction of influence depends on type of roughness, the operating parameter and on the nominal geometry. The effect of surface roughness with couple stress fluids on porous hydrodynamic bearings is examined by authors like Naduvinamani et al. [11, 12]. The effect of surface roughness on turbulent transonic flow over circular arc bumps in a channel is studied by Mendona and Sharif [13]. The effect of surface roughness on magneto hydrodynamic fluids is studied by Naduvinamani et al. [14] and Ramesh et al. [15]. Effects of scale and surface roughness on efficiency of water jet pumps using CFD is studied by Aldas and Yapici [16]. The influences of longitudinal surface roughness on sub-critical and super-critical limit cycles of short journal bearings is studied by Jaw- Ren Lin [17]. Amira Amamou and Mnaouar Chouchane [18] investigated nonlinear stability analysis of long hydrodynamic journal bearing using numerical continuation. It was found that the stability threshold occurs either at super critical or at a subcritical Hopf bifurcation depending on bearing characteristics. Tze-Chi Hsu et al. [19] investigated the study effects of magnetic field and surface roughness on infinitely long journal bearing. It was shown that due to the magnetization and surface roughness performance of bearing characteristics was improved.

In traditional lubrication theory, no-slip boundary condition is taken as basic foundation but researchers have found that no-slip boundary condition is not applicable for the special engineered surface, because it is found that slip occurs at the interface. The effects of engineered slip/no-slip on bearing surface by considering heterogeneous pattern (which means slip occurs in one region and is absent in other) have been studied by Salant and Fortier [20, 21, 22, 23]. In all these analysis, it is assumed that the bearing surfaces are smooth but it is not realistic. Recently, Kalavathi et al. [24, 25] have extended the effect of surface roughness on infinitely short and finite porous journal bearing by considering heterogeneous surface. It was found that roughness effect improves performance of bearing characteristics.

Here, it is assumed that fluid slip is occurring in accordance with Navier relation [26] and also the critical value of shear stress before slip onset may be considered which is suggested by Zhu and Granic [27]. An assumption of conventional lubrication theory is used. Also, porous matrix is assumed to be homogeneous, isotropic and

flow is governed by Darcys law. Stochastic theory of Christensen is used to study the effect of roughness. The effect of surface roughness is numerically studied on journal bearing surface with heterogeneous slip/no-slip surfaces. As an illustration, the lubricant flow along the axis of journal is neglected, i.e., the flow is considered only along circumferential direction. The aim of current work is to find out the effects of roughness and the porosity on heterogeneous surface in case of infinitely long journal bearing.

2. ANALYSIS

Fig.1 shows the diagram of journal bearing geometry and the heterogeneous slip/no-slip pattern is shown in Fig.2. The film thickness distribution is shown in Fig.2(a). Here, two surfaces are present, surface 1 represent moving shaft with speed, u_s and surface 2 represents bearing sleeve, which is stationary. Fig.2(b) shows the slip/no-slip pattern i.e., heterogeneous pattern is applied on the surface 2. The modified Reynolds equation for longitudinal and transverse roughness along circumferential direction by considering Navier slip boundary condition [26] and porous wall thickness (Prakash and Vij, [28]) by following Kalavathi et al.[24] is expressed as

$$\begin{aligned} \frac{d}{d\theta} [\{E(\bar{H}^3(1 + 3\Sigma)) + 12kH_0\} \frac{d}{d\theta} \{E(P)\}] \\ = 6\mu u_s R \frac{d}{d\theta} E\{\bar{H}(1 + \Sigma)\} \end{aligned} \quad (1)$$

for longitudinal roughness.

$$\begin{aligned} \frac{d}{d\theta} [\{ \frac{1}{E(1/\bar{H}^3(1 + 3\Sigma))} + 12kH_0\} \frac{d}{d\theta} \{E(P)\}] \\ = 6\mu u_s R \frac{d}{d\theta} \left\{ \frac{(1 + \Sigma)/\bar{H}^2(1 + 3\Sigma)}{E\{1/\bar{H}^3(1 + 3\Sigma)\}} \right\} \end{aligned} \quad (2)$$

for transverse roughness.

Here $\bar{H} = \Delta r(1 + \varepsilon \cos\theta) + h_s$ and $E(\)$ is the expectancy operator given by

$$E(\square) = \int_{-\infty}^{\infty} (\square) f(h_s) dh_s,$$

where $f(h_s)$ is the probability density distribution function of the stochastic variable h_s and is defined as

$$f(h_s) = \begin{cases} \frac{35}{32c^7} (c^2 - h_s^2)^3, & -c < h_s < c \\ 0, & elsewhere \end{cases}$$

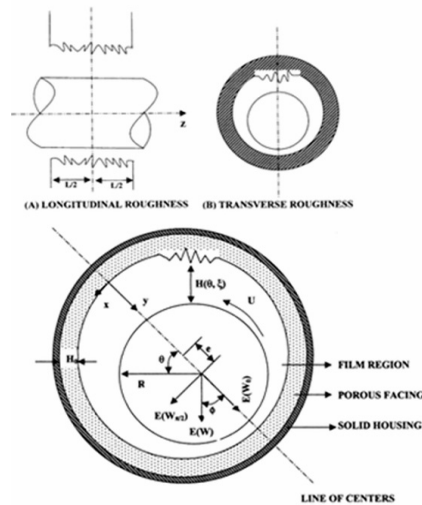


Fig. 1 Bearing geometry and journal bearing configuration.

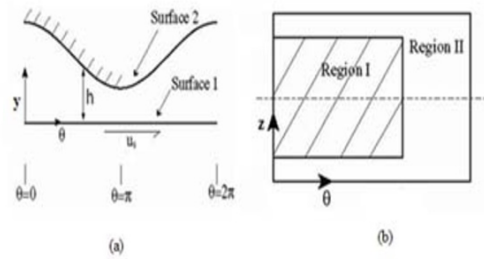


Fig. 2 (a) Diagram of journal bearing in cartesian coordinate configuration.
 (b) Diagram of surface pattern applied to Surface 2

The boundary conditions for pressure are

$$E(p) = 0 \quad \text{at} \quad \theta = 0 \quad (3)$$

$$\frac{d}{d\theta} E(p) = 0 \quad \text{at} \quad \theta = \theta_2 \quad (4)$$

where θ_2 is the angular extent of the film.

2.1. Longitudinal Roughness

The equation (1) is solved for dimensionless mean pressure \bar{p} by integrating with respect to θ twice and subjecting to the boundary conditions of equations (3) and (4),

$$\bar{p} = \frac{E(P)\Delta r^2}{\mu u_s R} = \int_0^\theta \frac{6[\{\bar{H}(1+\Sigma)\} - \{\bar{H}(1+\Sigma)\}_{\theta=\theta_2}]}{[\bar{H}^3(1+3\Sigma) + 12\psi]} d\theta \quad (5)$$

where $\psi = \frac{kH_0}{\Delta r^3}$, $\Sigma = \frac{A}{(H+A)}$, is the permeability parameter. In equation (5), $A \rightarrow 0$ corresponds to case studied by Gururajan and Prakash [6]. The angle θ at which the oil film breaks and the cavitation region start is calculated by adopting Reynolds condition

$$\bar{p}(\theta_2) = 0. \quad (6)$$

By equating equation (5) to zero and simplifying, we obtain

$$-(G_6)_{\theta_2} \int_0^{\theta_2} \frac{d\theta}{\{G_7 + 12\psi\}} + \int_0^{\theta_2} \frac{G_6 d\theta}{\{G_7 + 12\psi\}} = 0 \quad (7)$$

The expressions for G-functions are given in appendix. The average load along the line of center is as follows

$$E(W_0) = E(W)\cos\phi = -LR \int_0^{\theta_2} E(p)\cos\theta d\theta \quad (8)$$

The non-dimensional form of equation (8) is

$$\bar{W}_0 = \frac{E(W_0)\Delta r^2}{\mu u_s LR^2} = - \int_0^{\theta_2} \bar{p}\cos\theta d\theta \quad (9)$$

The average load along normal to the line of center is as follows

$$E(W_{\Pi/2}) = E(W)\sin\phi = LR \int_0^{\theta_2} E(p)\sin\theta d\theta \quad (10)$$

Dimensionless form of equation (10) is

$$\bar{W}_{\Pi/2} = \frac{E(W_{\Pi/2})\Delta r^2}{\mu u_s LR^2} = \int_0^{\theta_2} \bar{p}\sin\theta d\theta \quad (11)$$

The total dimensionless load carrying capacity is given by

$$W^* = \frac{E(W)\Delta r^2}{\mu u_s LR^2} = \sqrt{\bar{W}_0^2 + \bar{W}_{\Pi/2}^2} \quad (12)$$

Attitude angle is given by [6]

$$\phi = \tan^{-1}\left(\frac{\bar{W}_{\Pi/2}}{\bar{W}_0}\right) \quad (13)$$

The expression for average circumferential frictional force on the surface of journal at $y = H$ is as follows [6]

$$E(F) = \int_{-L/2}^{L/2} \int_0^{2\Pi} E(\tau_H) R d\theta dz \tag{14}$$

where τ_H is given by

$$\tau_H = \frac{1}{2} \frac{\partial p}{\partial x} \frac{H^2}{(H + A)} + \mu u_s \frac{1}{(H + A)}. \tag{15}$$

Taking expectation on both sides of equation (15) and then integrating,

$$\begin{aligned} E(F) = LR \int_0^{\theta_2} \frac{1}{2} E\left(\frac{\bar{H}^2}{\bar{H} + A}\right) \frac{\partial E(P)}{\partial \theta} d\theta \\ + \mu u_s LR \int_0^{\theta_2} E\left(\frac{1}{\bar{H} + A}\right) d\theta \\ + \mu u_s LR \int_{\theta_2}^{2\Pi} \left[\frac{\bar{h}_{\theta_2}}{\bar{h}}\right] E\left(\frac{1}{\bar{H} + A}\right) d\theta \end{aligned} \tag{16}$$

The non-dimensional frictional force is given by

$$\begin{aligned} F^* = \frac{E(F)\Delta r}{\mu u_s LR} = \int_0^{\theta_2} \frac{1}{2} G_8 \frac{d\bar{p}}{d\theta} d\theta + \int_0^{\theta_2} G_2(\bar{h} + A, C) d\theta \\ + \int_{\theta_2}^{2\Pi} \left[\frac{\bar{h}_{\theta_2}}{\bar{h}}\right] G_2(\bar{h} + A, C) d\theta, \end{aligned} \tag{17}$$

$$\text{where, } \frac{d\bar{p}}{d\theta} = \frac{6[G_6 - (G_6)\theta_2]}{G_7 + 12\psi} \tag{18}$$

The ratio of mean frictional force and mean load carrying capacity gives coefficient of friction μ^* .

2.2. Transverse Roughness

Equation (2) is solved for mean pressure \bar{p} , by integrating twice with respect to θ and subjecting to the boundary conditions given in equation (3) and (4),

$$\bar{p} = \frac{E(P)\Delta r^2}{\mu u_s R} = \int_0^\theta \frac{\left\{ \left(\frac{G_9}{G_{10}}\right) - \left(\frac{G_9}{G_{10}}\right)_{\theta=\theta_2} \right\}}{\left\{ \left(\frac{1}{G_{10}}\right) + 12\psi \right\}} d\theta \tag{19}$$

The cavitation angle θ_2 is given by

$$-\left(\frac{G_9}{G_{10}}\right)_{\theta=\theta_2} \int_0^{\theta_2} \frac{G_{10} d\theta}{\{1 + 12\psi G_{10}\}} + \int_0^{\theta_2} \frac{G_9 d\theta}{\{1 + 12\psi G_{10}\}} = 0 \tag{20}$$

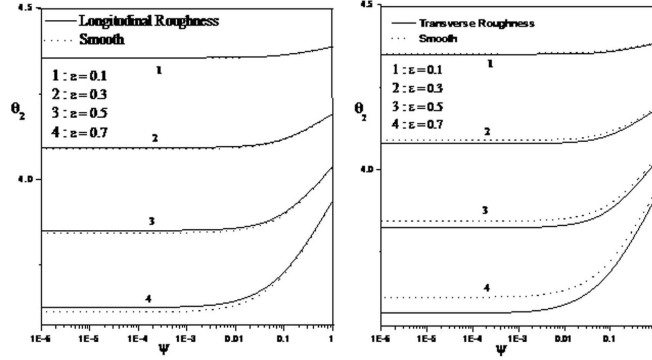


Fig. 3. Angle of cavitation θ_2 versus permeability parameter ψ for various values of eccentricity ratio ε with $C=0.2$ and $A=3$.

The dimensionless load carrying capacity can be obtained by substituting the pressure from equation (19) in equations (9) and (11). Mean load capacity is obtained by equation (12) and attitude angle is given by equation (13).

The mean circumferential frictional force acting on the journal surface at $y = H$ is given by

$$\begin{aligned}
 F^* &= \frac{E(F)\Delta r}{\mu u_s LR} \\
 &= -\frac{1}{6A} \int_0^{\theta_2} \frac{d\bar{p}}{d\theta} \left\{ \frac{G_{11} - G_2(\bar{h}, C)}{G_{10}} \right\} d\theta \\
 &\quad + \frac{1}{A} \int_0^{\theta_2} \left[G_{12} \left\{ \frac{G_{11} - G_2(\bar{h}, C)}{G_{10}} \right\} \right. \\
 &\quad \left. + \left\{ G_{13} - G_{14} + AG_2(\bar{h} + A, C) \right\} \right] d\theta \\
 &\quad + \frac{1}{A} \int_{\theta_2}^{2\pi} \left[\frac{\bar{h}_{\theta_2}}{\bar{h}} \right] \left[G_{12} \left\{ \frac{G_{11} - G_2(\bar{h}, C)}{G_{10}} \right\} \right. \\
 &\quad \left. + \left\{ G_{13} - G_{14} + AG_2(\bar{h} + A, C) \right\} \right] d\theta \\
 &\quad \text{where, } \frac{d\bar{p}}{d\theta} = \frac{6 \left[\left(\frac{G_9}{G_{10}} \right) - \left(\frac{G_9}{G_{10}} \right)_{\theta_2} \right]}{\left[\left(\frac{1}{G_{10}} \right) + 12\psi \right]}
 \end{aligned} \tag{21}$$

$$\tag{22}$$

The coefficient of friction,

$$\mu^* = \frac{F^*}{W^*} \tag{23}$$

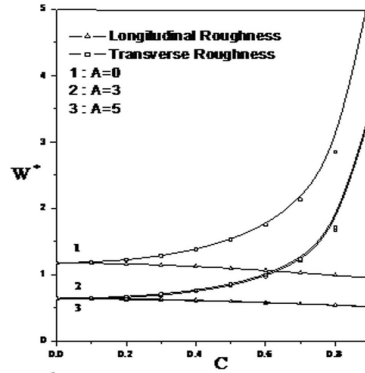


Fig. 4. Non-dimensional mean load capacity W^* verses roughness parameter C for different values of slip parameter A with $\psi = 0.01$ and $\varepsilon = 0.1$.

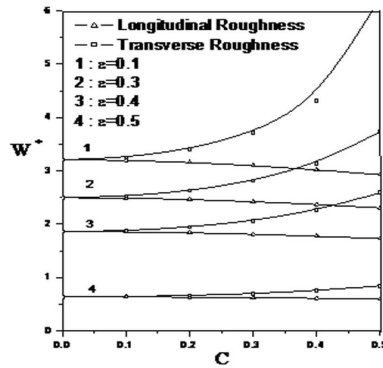


Fig. 5. Non-dimensional mean load capacity W^* verses roughness parameter C for different values of eccentricity ratio ε with $\psi = 0.01$ and $A=5$.

3. RESULT AND DISCUSSION

The dimensionless bearing characteristics are expressed as the function of roughness height by roughness parameter $C = c/\Delta r$, bearing eccentricity by the eccentric ratio $\varepsilon = e/\Delta r$, porosity by the permeability parameter $\psi = \Phi H_0/(\Delta r)^3$ and the slip coefficient by the parameter $A = \alpha\mu/\Delta r$.

Numerical results are illustrated in graphs. The definite integrals appearing in various expressions of bearing characteristics are evaluated by using 16 - point Gauss quadrature formula. The values chosen for the various parameters are as follows: ε is ranging from

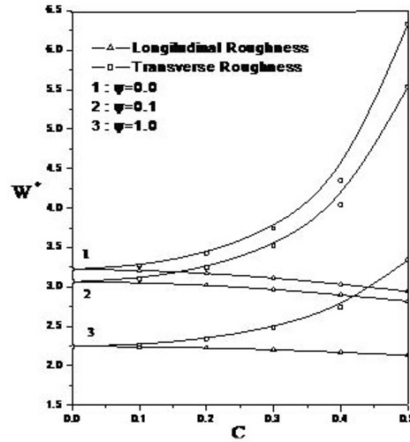


Fig. 6. Non-dimensional mean load capacity W^* verses roughness parameter C for different values of permeability parameter ψ with $\varepsilon = 0.5$ and $A=5$.

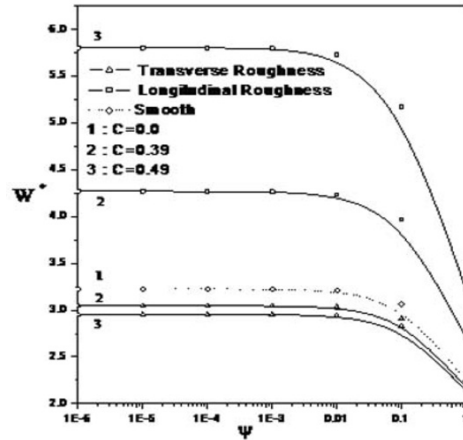


Fig. 7. Non-dimensional mean load capacity W^* verses permeability parameter ψ for different values of C with $\varepsilon = 0.5$ and $A=5$.

0.1 to 0.9, $\psi = 0, 0.001, 0.01, 0.1, 1$. The values used here cover all the ranges of industry practice shown by Murti [29]. $\psi = 0$ represents non porous bearing. C takes the values from 0.1 to 0.9. The values of slip parameter A is ranging from 0, 3, 5, 10 (Salant and Fortier, [23]). $C=0$ and $A=0$ represents smooth bearing (the case studied by Prakash and Vij, [30]). $A=0$ represents no-slip surface studied by Gururajan and Prakash [6]. Journal bearing are commonly used in rotating machines like pumps, home appliances, automobiles, generators and etc..

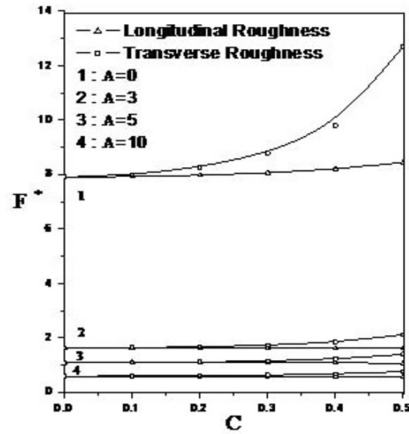


Fig. 8. Non-dimensional mean frictional force F^* verses roughness parameter C for different values of A with $\varepsilon = 0.5$ and $\psi = 0.01$.

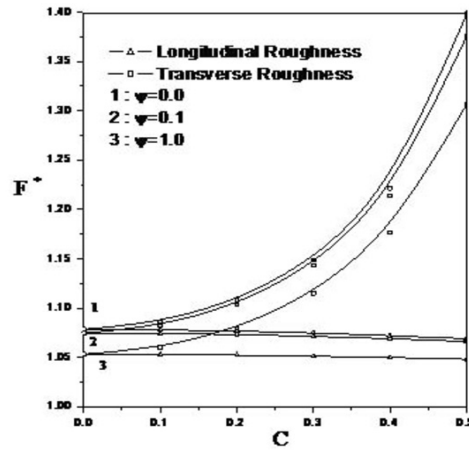


Fig. 9. Non-dimensional mean frictional force F^* verses roughness parameter C for different values of ψ with $\varepsilon = 0.5$ and $A = 5$.

The roughness effects is studied by considering its effect on lubrication flow (i.e., bearing is running hydrodynamically). When the heights of surface roughness are more than minimum film thickness the assumption made is invalid. Therefore, the mean oil film thickness should be less than 3δ for the bearing to operate hydrodynamically. This is possible when the values of C are less than $1-\varepsilon$. This study says that for the better performance of bearing, a suitable value of roughness parameter, eccentricity ratio and slip

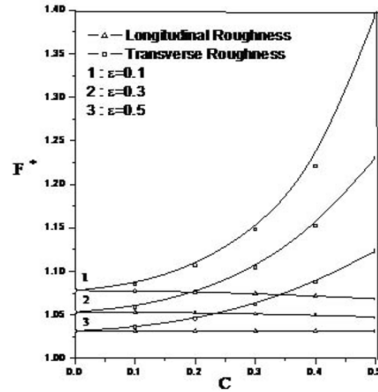


Fig. 10. Non-dimensional mean frictional force F^* versus roughness parameter C for different values of ε with $\psi=0.01$ and $A=5$.

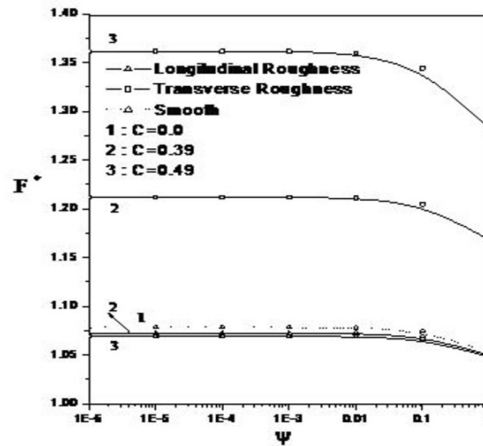


Fig. 11. Non-dimensional mean frictional force F^* versus permeability parameter ψ for different values of C with $\varepsilon=0.5$ and $A=5$.

parameter should be selected. In practical, to improve bearing performance slip parameter be kept minimum.

3.1. Angular Extent of Oil Film: Fig.3 describes the angular extent of the fluid film θ_2 for different values of eccentricity ratio with fixed slip parameter and roughness parameter. The roughness parameter is fixed for $C=0.2$ this is because the maximum peak-to-peak roughness is 20% of the diametral clearance of the bearing. It is observed that transverse roughness causes a slight decrease in θ_2

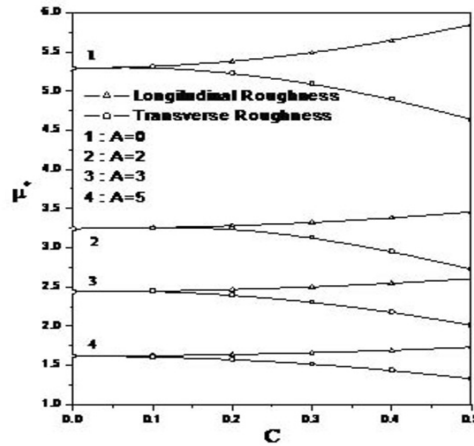


Fig. 12. Non-dimensional coefficient of frictional force μ^* versus roughness parameter C for different values of A with $\varepsilon=0.5$ and $\psi=0.01$.

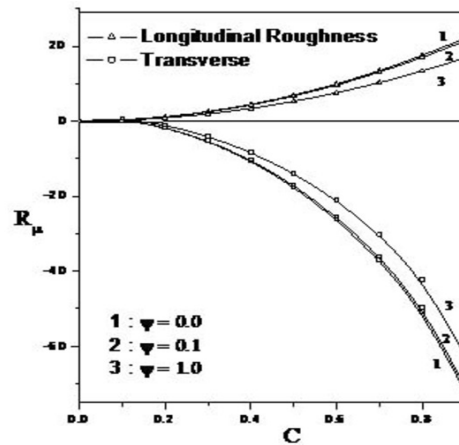


Fig. 13. Relative difference R_μ in mean coefficient of frictional versus roughness parameter C for different values of ψ with $\varepsilon=0.1$ and $A=3$.

when compared with smooth bearing, whereas longitudinal roughness results in an increase in θ_2 . This behavior is observed for all the values of ε and the effect of roughness is significantly high for higher values of ε and lower values of ψ . These changes are due to the presence of roughness which causes the altered flow of lubricant. Increasing value of ψ results in an increase of θ_2 which means that the cavitation region is reduced by increasing permeability, with other parameters being fixed. The similar effect is found in the

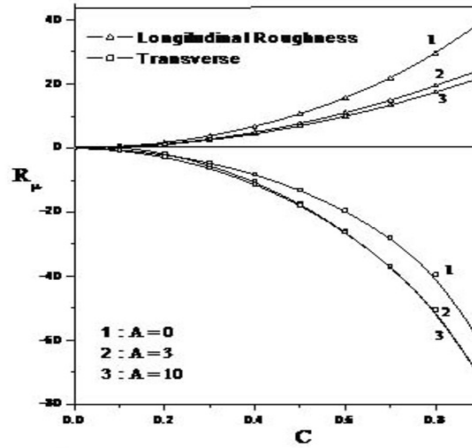


Fig. 14. Relative difference R_μ in mean coefficient of frictional verses roughness parameter C for different values of A with $\epsilon=0.1$ and $\psi=0.01$.

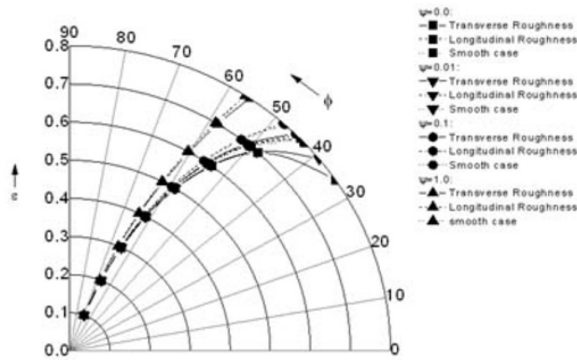


Fig. 15. Attitude angle ϕ verses eccentricity ratio ϵ for various values of ψ with $C=0.2$ and $A=3$.

journal of Gururajan[6] graphs.

3.2. Load Carrying Capacity: The results of non dimensional mean load carrying capacity are presented in Fig.4 through Fig.7. Figs.4, 5 and 6 shows the variation of load capacity as function of the roughness parameter C for different values of A , ϵ and ψ respectively for both types of roughness patterns. Corresponding to the hydrodynamic limit, the curves in Fig.4 are terminated at $\epsilon=0.1$ and $C=0.9$. It is observed that the effect of transverse roughness

increases the load for various values of slip coefficient A whereas, longitudinal roughness decreases load as compared to smooth one. When compared to slip surface, load is significantly higher for no-slip surface ($A=0$). Once slip parameter is larger than three, variation in A has an insignificant effect on the performance of bearing.

Fig.5 contains the graph of load with roughness parameter for different values of ϵ with fixed ψ and A . It is observed that transverse roughness increases the load carrying capacity but longitudinal roughness slightly decreases the load. Also, as eccentricity increases load carrying capacity decreases.

Fig.6 shows the plot of load carrying capacity verses roughness for various values of ψ with fixed ϵ and A . In this case transverse roughness increases the load carrying capacity but longitudinal roughness decreases the load. It is more significant for transverse roughness. Also, as permeability increases the load capacity decreases.

Thus the roughness effect strongly depends on surface texture. Both the types of roughness have an opposite influence. This is because the load capacity is induced by the alteration flow due to the presence of roughness as seen in report of Gururajan [6, 8].

The variation of W^* with ψ for different values of roughness parameter is shown in Fig.7. For $C=0.49$, a large scale increase in load with transverse roughness is seen when compared to longitudinal. The roughness effect decreases load with increasing values of ψ . Large permeability means there are more voids available in porous facing, for the quick escape of fluid and porous facing is main channel for the fluid discharge, therefore the modification of film thickness have negligible effect due to the presence of surface roughness. This result is also in accordance with the fact that for higher values of permeability the resistance offered by fluid film is very small. Therefore the roughness effect for a fixed value of C decreases with increase of ψ .

3.3. Frictional Force: Figs. 8, 9, 10 and 11 shows the variation of non-dimensional friction force. It is seen that roughness always increases the friction as compared to smooth. This is due to the fact that for the rough surface, the Couette friction component is always greater when compared with a smooth surface and as $(C + \epsilon) \rightarrow 1$, effect will be more accentuated.

Fig. 8 illustrates the effect of roughness on frictional force for various values of A with fixed eccentricity and permeability. In accordance with smooth case, it is noted that roughness increases

the frictional force for transverse roughness whereas this significant is very less for longitudinal. Also, frictional force decreases with increasing values of slip parameter. It is seen that, plot of $A=0$ is similar to the graph of Gururajan and Prakash [6].

The graph of F^* with C for various values permeability factor with fixed slip parameter and eccentric ratio is depicted in Fig. 9. As roughness increases the frictional force increases. The curve is more significant for transverse roughness whereas slight decrease is observed for longitudinal roughness. Frictional force decreases with increase of permeability.

Fig.10 contains a plot of mean friction as a roughness parameter for various eccentricity values with fixed slip parameter and permeability. Decrease in friction is observed for longitudinal roughness whereas friction significantly increases with roughness for the bearing with transverse roughness structure. Frictional force decreases with increase of eccentricity.

The friction as a function of permeability for the selected values of C parameter is drawn. This shows that friction decreases with an increase in ψ for both types of roughness. This will be more pronounced for transverse roughness especially for the values of C approaching the hydrodynamic limit $C=0.49$ and $\epsilon=0.5$ see the Fig.11.

From these figures, it is evident that for longitudinal roughness, the effect is less significant as compared with smooth one. In practical case, friction is regarded as insensitive to one dimensional longitudinal roughness. For transverse roughness pattern, substantial increase in friction is observed in correspondence with smooth, because of increase of Couette part of friction component and Poiseuille component.

3.4. Coefficient of Friction: Fig.12 is a graph of variation of μ^* with C for several values of A . It can be identified that both types of roughness have an opposite influence. Longitudinal irregularity raises the friction coefficient with increase of roughness parameter whereas transverse roughness decreases. This is partly because of increasing friction and decreasing load.

The roughness effect on the surface of bearing is calculated by relative difference coefficient R_μ , where $R_\mu = \left(\frac{\mu_{rough}^* - \mu_{smooth}^*}{\mu_{smooth}^*} \right) X 100$.

Fig.13 and Fig.14 shows the coefficient of friction as a function of roughness for different values of permeability and slip parameter respectively. It is observed that coefficient of friction increases with

roughness for longitudinal type and it decreases for transverse case. The effect will be almost independent of variations in permeability and slip.

3.5. Attitude Angle: Fig.15 shows the locus of the journal centre for various values of ψ with fixed roughness parameter and slip parameter. It is observed that roughness effects are not very much significant, although attitude angle varies appreciably with ψ . Attitude angle decreases as compared to smooth for transverse roughness. But the effects are never significant for longitudinal roughness.

4. CONCLUSION

This study indicates that effect of roughness on a bearing surface with heterogeneous slip/no-slip can improve the performance of journal bearing and the direction of influence depends on type of roughness.

A transverse roughness hampers the flow, this results in significant increase in load carrying capacity and friction. However, coefficient of friction is decreased. The effect of roughness strongly depends on eccentricity and permeability. Also, ϕ decreases slightly with increase of ε when compared to smooth.

A longitudinal roughness will ease out the outflow of lubricant, thereby decreasing the load capacity. However, slight increase in friction force and coefficient of friction are observed. Friction force is weakly depending on permeability. Notably, ϕ is not altered much.

ACKNOWLEDGEMENTS

The authors are grateful to the Malnad College of Engineering, Hassan and M S Ramaiah Institute of Technology, Bangalore for all the support and also the financial support from Visvesvaraya Technological University research scheme project No. VTU/Aca./2010-11/A-9/11547.

NOMENCLATURE

A	dimensionless slip coefficient $\alpha\mu/\Delta r$
C	dimensionless roughness parameter ($= c/\Delta r$)
c	maximal asperity deviation from the nominal film height
E()	expected value of

e	bearing eccentricity
F^*	mean frictional force ($= E(F)\Delta r/\mu URL$)
f^*	coefficient of friction ($= (R/\Delta r)E(F)$)
H	film thickness ($= h + h_s$)
\bar{H}	nominal fluid film
H_o	thickness of porous bearing height ($= H/\Delta r$)
h	nominal film height ($= (\Delta r)(1 + \cos\theta)$)
\bar{h}	film height ($= h/\Delta r$)
h_s	deviation of film height from the nominal level
k	permeability
L	bearing length
p	pressure in the film thickness
\bar{p}	mean pressure ($= \{(E(p)\Delta r^2)/\mu u_s R\}$)
R	journal radius
$R_{()}$	relative difference (<i>e.g.</i> , $R_W = (\{W_r^* - W_s^*\}/W_s^*)X100$)
u,v,w	velocity components in the film thickness
u_s	Shaft surface speed
V_o	normal velocity of the lubricant at the Bearing interface with which it is getting into Pores
W	load capacity
$W_o, W_{(\Pi/2)}$	load components
W^*	mean load capacity ($= [\{E(w)(\Delta r)^2\}/(u_s R^2 L)]$)
x,y,z	Cartesian co-ordinates
α	slip coefficient
σ	standard deviation
ε	eccentricity ratio ($= e/\Delta r$)
μ	viscosity of the lubricant
θ	circumferential co-ordinate ($x = R$)
Δr	radial clearance
ξ	random variable
Σ	$A/(\bar{H} + A)$

APPENDIX

The various G - functions are given as follows

$$\begin{aligned}
 \text{A1} \quad & E(\bar{H}) = \bar{h} = 1 + \varepsilon \cos\theta. \\
 \text{A2} \quad & E(\bar{H}^2) = \bar{h}^2 + C^2/9. \\
 \text{A3} \quad & E(\bar{H}^3) = \bar{h}^3 + \bar{h}C^2/3. \\
 \text{A4} \quad & G_2(\bar{h}, C) = E\left(\frac{1}{\bar{H}}\right) = \frac{1}{\bar{h}} \left\{ 1 + 105 \sum_{n=1}^{\infty} \frac{X^{2n}}{(2n+1)(2n+3)(2n+5)(2n+7)} \right\}, \\
 \text{A5} \quad & G_3(\bar{h}, C) = E\left(\frac{1}{\bar{H}^2}\right) = \frac{1}{\bar{h}^2} \left\{ 1 + 105 \sum_{n=1}^{\infty} \frac{X^{2n}}{(2n+3)(2n+5)(2n+7)} \right\},
 \end{aligned}$$

$$\begin{aligned}
\text{A6} \quad G_4(\bar{h}, C) &= E\left(\frac{1}{\bar{H}^3}\right) = \frac{1}{\bar{h}^3} \left\{ 1 + 105 \sum_{n=1}^{\infty} \frac{(n+1)X^{2n}}{(2n+3)(2n+5)(2n+7)} \right\}, \\
&\text{where } X = \frac{c}{\bar{h}}. \\
\text{A7} \quad G_2(\bar{h} + A, C) &= E\left(\frac{1}{\bar{H} + A}\right) \\
&= \frac{1}{(\bar{h} + A)\frac{c}{\bar{h}}} \left\{ 1 + 105 \sum_{n=1}^{\infty} \frac{X^{2n}}{(2n+1)(2n+3)(2n+5)(2n+7)} \right\}, \\
&\text{where } X = \frac{c}{\bar{h} + A}. \\
\text{A8} \quad G_2(\bar{h} + 4A, C) &= E\left(\frac{1}{\bar{H} + 4A}\right) \\
&= \frac{1}{(\bar{h} + 4A)\frac{c}{\bar{h}}} \left\{ 1 + 105 \sum_{n=1}^{\infty} \frac{X^{2n}}{(2n+1)(2n+3)(2n+5)(2n+7)} \right\}, \\
&\text{where } X = \frac{c}{\bar{h} + 4A}. \\
\text{A9} \quad G_6(\bar{h}, A, C) &= E\{\bar{H}(1 + \Sigma)\} = E(\bar{H}) + A - A^2 G_2(\bar{h} + A, C) \\
&\text{Method to obtain expected values :} \\
&\bar{H}(1 + \Sigma) = \bar{H} \left(1 + \frac{A}{\bar{H} + A} \right) = \bar{H} + A - \frac{A^2}{\bar{H} + A} \quad (\text{By division}) \\
&E\{\bar{H}(1 + \Sigma)\} = E\left[\bar{H} + A - \frac{A^2}{\bar{H} + A} \right] \\
&= E(\bar{H}) + A - A^2 E\left(\frac{1}{\bar{H} + A}\right) \\
&= \bar{h} + A - A^2 G_2(\bar{h} + A, C) \\
\text{A10} \quad G_7(\bar{h}, A, C) &= E\{\bar{H}^3(1 + 3\Sigma)\} \\
&= E(\bar{H}^3) + 3AE(\bar{H}^2) - 3A^2 E(\bar{H}) + 3A^3 - 3A^4 G_2(\bar{h} + A, C). \\
\text{A11} \quad G_8(\bar{h}, A, C) &= E\left(\frac{\bar{H}^2}{\bar{H} + A}\right) = E(\bar{H}) - A + A^2 G_2(\bar{h} + A, C). \\
\text{A12} \quad G_9(\bar{h}, A, C) &= E\left(\frac{1 + \Sigma}{\bar{H}^2(1 + 3\Sigma)}\right) \\
&= \frac{1}{8A} \left\{ G_2(\bar{h}, C) - G_2(\bar{h} + 4A, C) \right\} + \frac{1}{2} G_3(\bar{h}, C). \\
\text{A13} \quad G_{10}(\bar{h}, A, C) &= E\left(\frac{1}{\bar{H}^3(1 + 3\Sigma)}\right) \\
&= \frac{3}{64A^2} \left\{ G_2(\bar{h} + 4A, C) - G_2(\bar{h}, C) \right\} + \frac{3}{16A} G_3(\bar{h}, C) + \frac{1}{4} G_4(\bar{h}, C). \\
\text{A14} \quad G_{11}(\bar{h}, A, C) &= E\left(\frac{1}{\bar{H}(1 + 3\Sigma)}\right) = \frac{1}{4} G_2(\bar{h}, C) + \frac{3}{4} G_2(\bar{h} + A, C). \\
\text{A15} \quad G_{12}(\bar{h}, A, C) &= \frac{d}{d\theta} E\left(\frac{1 + \Sigma}{\bar{H}^2(1 + 3\Sigma)}\right) \\
&= (-\varepsilon \sin\theta) \left[\frac{1}{8A} G_3(\bar{h} + 4A, C) - G_3(\bar{h}, C) - G_4(\bar{h}, C) \right]. \\
\text{A16} \quad G_{13}(\bar{h}, A, C) &= \bar{E}(1 + \Sigma) = 1 + AG_2(\bar{h} + A, C). \\
\text{A17} \quad G_{14}(\bar{h}, A, C) &= E\left[\frac{(1 + \Sigma)}{(1 + 3\Sigma)}\right] = 1 - 2AG_2(\bar{h} + 4A, C).
\end{aligned}$$

REFERENCES

- [1] Tzeng S. T., and Saibel E., *Surface roughness effect on slider bearing lubrication*, Trans. ASME, J. Lub. Tech. **10**, 334-343, 1967.
- [2] Tzeng S. T., and Saibel E., *On the effect of surface roughness in the hydrodynamic theory of a short journal bearing*, Wear. **10**, 179-189, 1967.
- [3] Christensen H., *Stochastic model for hydrodynamic lubrication of rough surfaces*, Proceedings of the Institution of Mechanical Engineers, Part I 184 (56), 1013-102, 1969.
- [4] Patir N., and Cheng H.S., *Application of average flow model to lubrication between rough sliding surfaces*, ASME J. Lubr. Technol. **101**, 220-230, 1979.
- [5] Turga R., Sekhar A.S., Majumdar B.C., *The effect of roughness parameter on the performance of hydrodynamic journal bearing with rough surfaces*, Tribol Int. **32**, 231-236, 1999.

- [6] Gururajan K., and Prakash J., Majumdar B.C., *Surface roughness effects in infinitely long porous journal bearings*, ASME journal of tribology **121**, 139-47, 1999.
- [7] Prakash J., and Gururajan K., Majumdar B.C., *Effect of velocity slip in an infinitely long porous journal bearings*, Tribology Transaction. **2**, 661-667, 1999.
- [8] Gururajan K., and Prakash J., *Effect of surface roughness in a narrow porous journal bearing*, ASME Journal of Tribology. **122**, 472-475, 2000.
- [9] Gururajan K., and Prakash J. *Roughness effects in narrow porous journal bearing with arbitrary porous wall thickness*, Journal of Mechanical Sciences. **44**, 1003 - 1016, 2002.
- [10] Gururajan K., and Prakash J., *Effect of velocity slip in a narrow porous journal bearing*, Proceedings of the Institution of Mechanical Engineers, Part J: Journal of Engineering Tribology. **217**, 59 - 70, 2003.
- [11] Naduvinamani N.B., and Hiremath P.S., Gurubasavaraj G. *Surface roughness effects in a short porous journal bearings with a couple stress fluid*, Fluid Dynamic Research. **31**, 333- 354, 2002.
- [12] Naduvinamani N.B., and Hiremath P.S., Gurubasavaraj G. *Effects of Surface roughness on the static characteristics of rotor bearings with couple stress fluids*, Computer Structures. **80**, 1243 - 1253, 2002.
- [13] Mendona J., and M.A.R. Sharif. *Effect of surface roughness on turbulent transonic flow over circular arc bumps in a channel*, Engineering application of computational fluid mechanics. **4(2)**, 164-180, 2010.
- [14] Naduvinamani N.B., Hanumagouda B.N., Siddanagoud A. *Effect of Surface Roughness on Magneto-Hydrodynamic Couplestress Squeeze film Lubrication between Circular Stepped Plates*, *Lubrication Science*, John Wiley & Sons Ltd. **24(2)**, 61-74, 2012.
- [15] Ramesh B. Kudenatti, Shalini, M. Patil, Dinesh P.A. and Vinay C.V. *Numerical Study of Surface Roughness and Magnetic Field between Rough and Porous Rectangular Plates*, *Mathematical Problems in Engineering*. **13**, Article ID 915781, 2013.
- [16] Aldas K., and Yapici R. *Investigation of effects of scale and surface roughness on efficiency of water jet pumps using CFD*, Engineering application of computational fluid mechanics. **8(1)**, 14-25, 2014.
- [17] Jaw-Ren Lin. *The influences of longitudinal surface roughness on sub-critical and super-critical limit cycles of short journal bearings*, Applied Mathematical Modelling. **38(1)**, 392402, 2014.
- [18] Amira Amamou and Mnaouar Chouchane. *Nonlinear stability analysis of long hydrodynamic journal bearings using numerical continuation*, International journal of Mechanism and Machine Theory. **72** , 1724, 2014.
- [19] Tze-Chi Hsu, Jing-Hong Chen, Hsin-Lu Chiang and Tsu-Liang chou. *Combined effects of magnetic fluid and surface roughness on long journal bearing lubricated with ferrofluid*, J. marine science and tech. **22**, 154-162, 2014.
- [20] Salant R.F. *Numerical simulation of mechanical seal with an engineered slip/no slip surface* Proceedings of the 17th international conference on Fluid sealing, BHRG, Cranfield U.K **44**, 15-28, 2003.
- [21] Fortier A. *Numerical simulation of hydrodynamic bearings with engineered slip/no slip surfaces* M S thesis, Georgia Institute of Technology, Atlanta, GA, 2004.
- [22] Salant R.F., and Fortier A. *Numerical analysis of slider bearing with Heterogeneous slip/no-slip surface* Tribology Transaction. **47**, 328-334, 2004.
- [23] Salant R.F., and Fortier A. *Numerical analysis of Journal bearing with Heterogeneous slip/no-slip surfaces* Tribology Transaction. **127**, 820-825, 2005.
- [24] Kalavathi G.K., K. Gururajan, Dinesh P.A., Gurubasavaraj G. *Effect of surface roughness in a Narrow porous journal bearing with a heterogeneous slip/no-slip*

- surface* International journal of Scientific and Innovative Mathematical Research, **2(12)**,944-959, 2014.
- [25] Kalavathi G.K., Dinesh P.A., K. Gururajan *Influence of roughness on porous finite journal bearing with heterogeneous slip/ no-slip surface* Tribology International.**44**, 15-28, 2016.
- [26] Navier C. L. M. H. *Memoires de l Academic Royale des sciences de l Institute de France.* **1** , 414-416, 1823.
- [27] Zhu Yingxi, Steve Granick.*Rate Dependent Slip of Newtonian Liquids at Smooth Surfaces* Physical Review Letters 87.9: 096105, 1-4, (2001).
- [28] Prakash J., and Vij S K.*Analysis of narrow porous journal bearing using Beavers Joseph criterion of velocity slip* Trans. ASME J. Appl. Mechanics Series **41**, 348-353, 1974.
- [29] Murti P.R.K.*Effect of slip flow in narrow porous bearings with arbitrary wall thickness* ASME journal of applied mechanics**42(2)**, 305-310, 1975.
- [30] Prakash J., and Vij S.K.*Axially undefined porous journal bearing considering cavitation* Wear **22**, 1-14, 1972.

DEPARTMENT OF MATHEMATICS, MALNAD COLLEGE OF ENGINEERING, HASSAN, KARNATAKA, INDIA

E-mail addresses: kala.kgowda@gmail.com

DEPARTMENT OF MATHEMATICS, M. S. RAMAIAH INSTITUTE OF TECHNOLOGY, BANGALORE, KARNATAKA, INDIA

E-mail addresses: dineshdpa@msrit.edu

DEPARTMENT OF MATHEMATICS, MALNAD COLLEGE OF ENGINEERING, HASSAN, KARNATAKA, INDIA

E-mail addresses: kgururajan.hsn@gmail.com